70(8A): 1-479; 2022. DOI: 10.18311/jmmf/2022/32022

Print ISSN : 0022-2755
Journal of Mines, Metals and Fuels
Contents available at: www.informaticsjournals.com/index.php/jmmf

A Review on Understanding the Crystallization Process of Bioglass in Recent Decade

Shakthi Prasad P, Swetha B M and Prakrathi S*

*Biomaterials-Cluster Lab, Department of Mechanical Engineering, Ramaiah Institute of Technology, Bengaluru, India-560054. *E-mail: krathi.s@gmail.com*

Abstract

Bioglass is extensively used in clinical and bone tissue engineering, more specifically in orthopaedic as bone substitute in the form of granules or powders because of their excellent bioactivity, biodegradability and biocompatibility. They have the capability to form an integrated bond with bone through degradation and biomineralization at the surface of the living tissues. These activities are mainly driven by the composition, synthesis method and crystallinity of the bioglass. Therefore, in this paper we aimed at reviewing the basics and methods used in assessing the crystallization process of bioglasses and a few insights into crystallization revealed in the recent years. This critical review helps in tailoring and controlling crystallinity for their better applicability.

Keywords: *Bioglass, crystallization kinetics, Differential Scanning Calorimetry (DSC), X-Ray Diffraction Analysis (XRD), Microscopy.*

1.0 Introduction

Bioglass are the most effective implant materials that are applied in the reconstruction of bone tissues in tissue engineering and dental restorative, in the form of granules, powders, scaffolds, implants and coating [18-23]. These materials have excellent bioactivity, biocompatibility, osteoconductivity and osteoinductivity [13,20]. In which they are capable of forming an integrated bond between implant and bone tissue through biodegradation and biomineralization (i.e. hydroxyapatite) at the surface of the living tissue [13,23]. The rate of tissue bonding, strength and stability depends on the composition of Bioglass. Additionally, they are clinically applied in restoration of skeletal system which includes bones, joints and teeth [20].

The Bioglass was discovered by L.L. Hench et al. in 1969 at the University of Florida with composition (45% SiO_2, 24.5% CaO, 24.5% Na_2O, 6% P_2O_5) which was later termed as 45S5 Bioglass that are most widely investigated [5- 23]. Different types of Bioglass are being developed in recent decade such as silicates, borate and phosphate-based bioglasses. The production/preparation of Bioglass are carried out most frequently through traditional melt quenching method and sol gel method [23]. It is learnt from the literature that the biodegradation and biomineralization of bioglasses depends on the composition and structure [21]. The crystallization is a common event in bioglasses that occurs during annealing of melt quench scaffolds, sintering of quenched granules, stabilization and sintering of solgel processed bioglasses [26]. The main purpose of heat treatment is to eliminate the nitrates and other volatile compounds which comes from the precursor materials to have better control over the material composition, homogeneity, higher surface area,

*Corresponding author

enhanced bioactivity and introduction of functional metal elements for specific properties [1]. In case of solgel method bioglass devitrifies during this process, whereas the purpose of heat treatment in case of melt quench bioglass is to relief internal stress. Thus, during heat treatment the temperature and time directly effects the structure and bioactivity of the Bioglass [4]. Therefore, it is important to review and list the recent advances pertaining to this topic. Several studies have been reported in this decade on crystallization using Differential Scanning Calorimetry (DSC)/ Differential Thermal Analysis (DTA), Microscopic and X-Ray Diffraction (XRD) techniques.

2.0 Bioglass Synthesis

In melt-quench process initially precursors reagents such as SiO_2, Na_2CO_3, $CaCO_3$ and P_2O_5 are added and mixed together in platinum crucible and melted at 1300°C for 3 hours. Then, melt is quenched in water and dried at 120°C for 12 hours. After drying the bioglass is remelted for 1 hour to improve homogeneity and casted into block shape mold to obtain scaffolds [1]. Further, they are annealed at 480°C for 8 hours to remove internal stress. The main drawback of this method, it changes the composition of bioglass due to inducing at high temperature which results in volatilization of phosphate compound. So, the alternate method adapted to fabricate bioglass is solgel method, a type of wet-chemical technique. This method is the most effective way of producing the bioglass with low cost and at lower operational temperature [15].

The solgel method is the combination of hydrolysis, polycondensation of precursor materials through acid catalysis, solution gelation, aging, drying and heat treatment. Steps to obtain the 20gm yield of bioglass powder are as follows: initially 3.2ml of 69% nitric acid was added to 47.6ml of distilled water to get 1M nitric acid solution, 33.5ml of tetraethyl orthosilicate (TEOS) was added to the nitric acid solution and stirred for 1hr, 20.13g of calcium nitrate tetrahydrate, 2.9 ml of triethyl phosphate (TEP), 13.52g of sodium nitrate were added and stirred continuously for 45 minutes. Finally, a transparent solution was obtained and transferred to Teflon beaker, sealed with tin foil and stored in a ambient temperature to form a gel. Then, gel is aged for 24 hours at 60°C and dried at 120°C for 15 hours in hot air oven. Then bioglass powder were stabilized at different time and temperature [27]. Further, the crystallization studies can be performed on the obtained bioglasses.

3.0 Study of Crystallization Kinetics

The influence of time and temperature during the heat treatment leads to phase transformation from amorphous phase to crystalline phase which leads to the study of crystalline phases that are evolved. There are other factors affecting crystallinity such as glass composition, precursor materials, type of catalyst, aging time and particle size of the bioglass [30]. The Bioglass crystallizes between 600°C and 750°C as reported by Lefebver et al [9]. For example, the structural transformation in Bioglass occurs in 5 different stages, when the temperature reaches 550°C initial glass transition (Tg1) and 580°C glass in glass phase separation (Ts) occurs, this leads to creation of silica-rich and phosphate-rich phases. At 610°C, the primary crystallization of $Na_2CaSi_2O_6$ forms in silica-rich phase and at 800°C, crystallization of $Na_2Ca_4(PO_4)_2SiO_4$ forms in phosphate-rich phase. Further, at 850°C, glass transition 2(Tg_2) occurs to form full densification and at 1200°C, the bioglass melts [15]. In this work, the equation for activation energy of crystallization was determined using the Kissinger model i.e. equation (1),

$$\ln\left(\frac{\alpha^n}{Tp^2}\right) = -\frac{\mathrm{Ec}}{RTp} + C \quad \text{... (1)}$$

Where, α is the heating rate, Ec is the activation energy, R is the gas constant, T_p is the peak crystallization temperature, and C is the constant. The crystallization kinetics of phase transformation are often studied by using Avrami equation is given by (2):

$$n = \frac{2.5}{\Delta\tau}\frac{RTp^2}{Ec} \quad \text{... (2)}$$

Where $\Delta\tau$ is the full width of half maximum peak (FWHP), (Tp) is the peak temperature, α is constant heating rate that are taken from the DSC plots [9].

Prakrathi et.al. reported that nucleation and growth of crystalline phases are diffusion- controlled reactions and are governed by Arrhenius equation-based kinetics (3).

$$A = Ao * \exp^{\left(-\frac{E}{RT}\right)} \quad \text{... (3)}$$

Where, A is the rate constant, Ao is the exponent factor, E is the activation energy, R is the universal gas constant and T is the temperature. Thus, the rate constant (A) can be obtained from the slope of the curve fit from the graph –ln(1–X) v/s reaction time (t) at a constant temperature, (where, X is the crystalline fraction) and the activation energy of crystallization is obtained from the slope of the plot in (A) versus 1/RT,

the values for A are obtained at different reaction temperatures [27]. In the paper by Kashyap et.al., the changes in volume crystalline phase with respect to time is described using Avrami equation and the crystallization kinetic is obtained by using the below equation (4).

$$f = 1 - \exp(-kt^n) \quad \text{... (4)}$$

Where, f is the crystalline volume fraction, t is the time, k is the rate constant, n is the Avrami exponent. Referring to the above equation (4), the curve fit –ln (1 –f) v/s t gives "n" Avrami exponent, which specifies the type of crystallization that varies, if n=1 it is predominately surface crystallization, (1>n<3) then it is of both surface and volume crystallization, if n=3 it is volume crystallization. The slope of curve gives the rate constant of the reaction [26, 27].

3.1 Methods to Evaluate Crystallization Kinetics

3.1.1 Differential scanning calorimetry (DSC)

Bretcanu et.al. has carried experiments to monitor the thermal characteristic of bioglass, such as, glass transition temperature (T_g), crystallization temperature (T_c), and mass loss changes, 20mg of glass powder was heated in platinum crucible up to 1000°C with heating rate of 10°C/min and found that mass loss takes place in stages, from Fig.1, (i) from 22°C to 399°C with residual mass of 90.72%, and (ii) from 400°C to 1000°C with residual mass of 59.53% [18]. It was reported that crystallization occurred at a temperature range of 600°C to 853°C for both solgel and melt derived bioglasses, further, the glass transition temperature (Tg) and sharp exothermic peaks were occurred at 550°C and 703°C, respectively, for solgel derived Bioglass. The glass transition temperature (Tg) and exothermic peaks for melt derived Bioglass were occurred at 585°C and 795°C, respectively. Increasing the temperature up to 750°C led to 43wt.% crystalline fraction of bioglass [18]. Meszaros et.al. reported that, the crystalline phases, combeite and wollastonite. ($CaSiO_3$) phases were detected from DSC peaks at 795°C and 896°C, respectively [18]. The enthalpy of crystallization and activation energy for crystallization of combeite was determined using Kissinger method and Avrami exponent 'n' and found that n<1 which indicates that combeite phase occurs mainly on the surface of the bioglass. Before the heat treatment, the DSC curve found out that bioglasses contains both endothermic and exothermic peaks [1].

The Bioglass crystallization kinetics were directly

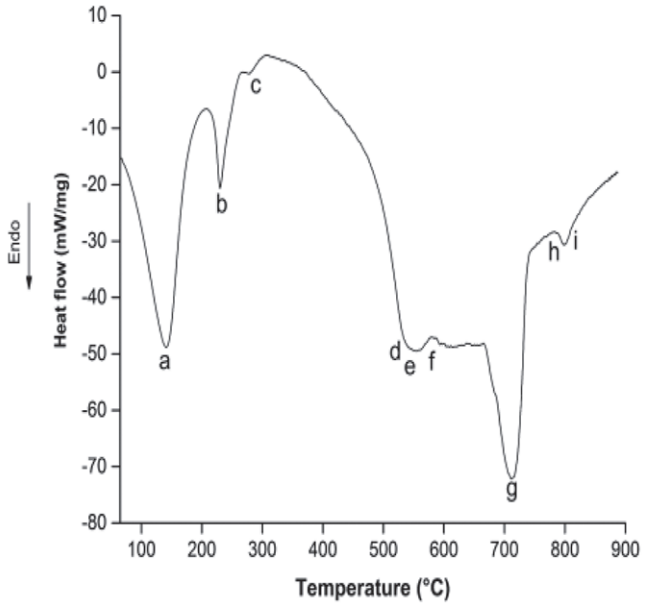

Figure 1: DSC of bioglass powder showing two major mass loss stages: (i) from 22°C to 399°C, (ii) from 400°C to 1000 °C, with residual mass respectively [24]

determined by DTA plots, the powder was heated at different rates, ranging from 5°C/min to 30°C/min, all curves showed large exothermic peaks at 600°C to 750°C and small endothermic peaks at 1150°C to 1250°C. From the obtained DTA plots (Figs.2 and 3), the glass transition temperature, onset crystallization temperature, activation energy at glass transition region and crystallization region can be determined, so that we can relate the amount of thermal energy required by the bioglass to flow through transition region. Once it is flowing the energy will decrease constantly until new crystallinities are formed which results in increased glass viscosity. The activation energy of crystallised bioglass was found to be lower than glass transformation region due to decrease in flow viscosity [24].

3.1.2 Microscopy characterisation

The microscopic analysis technique is used to study the evolution of microstructure during sintering and crystallization of the bioglass, since both porosity and crystallinity can be controlled during heating, major transformation occurs at this stage, and it effects the final properties. The parameters that influence the mechanical and biological behaviours are the size and amount bioglass. The amount of micropores in the bioglass leads to different surface topographies that influence the cell adhesion. The

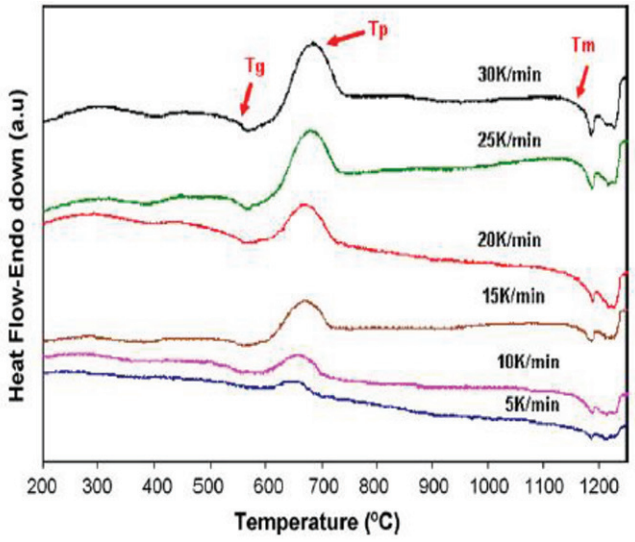

Figure 2: DTA curves obtained for Bioglass powder at different heating rates. [18]

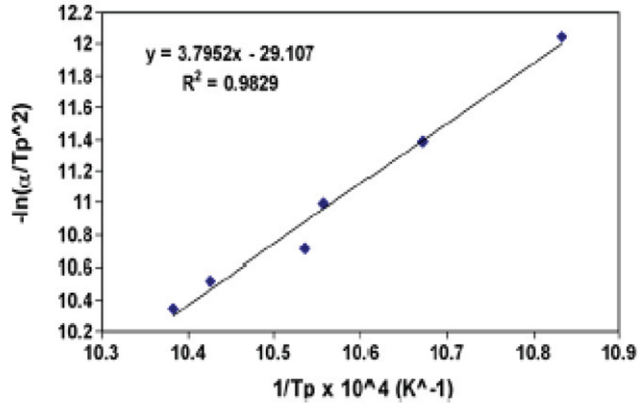

Figure 3: Calculation of the activation energy for crystallisation from DTA results, [–ln (α/T2p)] versus 1/Tp is represented above [18]

amount of macropores in the bioglass controls the penetration of fluids that affects the crystallinity of the bioglass. Therefore, glass-ceramic microstructures may control the bioactivity [26]. Optical microscopy (Figs.4 and 5) revels amorphous and partially crystallized bioglass at low magnification, that provides the evidence to support mechanism of degradation, which involves in glass-crystal interface [9]. The crystallization kinetics is studied using Avrami equation (4). The crystallization fraction formed v/s crystallinity time was graphically plotted by using the equation $f = 1 - \exp(-kt^n)$. The rate constant and Avrami exponent (n) were obtained when n~3 and

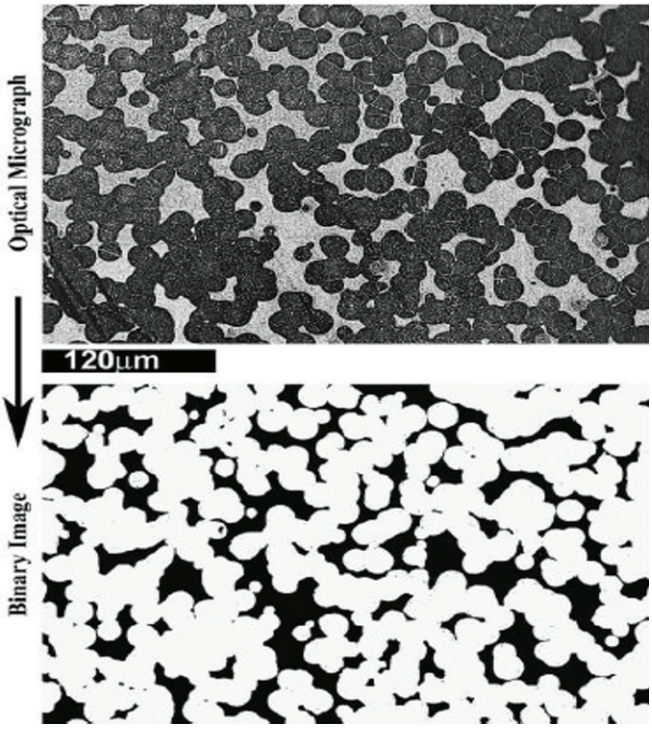

Figure 4: Initial conversion of optical micrograph to image. (Before using image for crystalline area fraction calculation)[26]

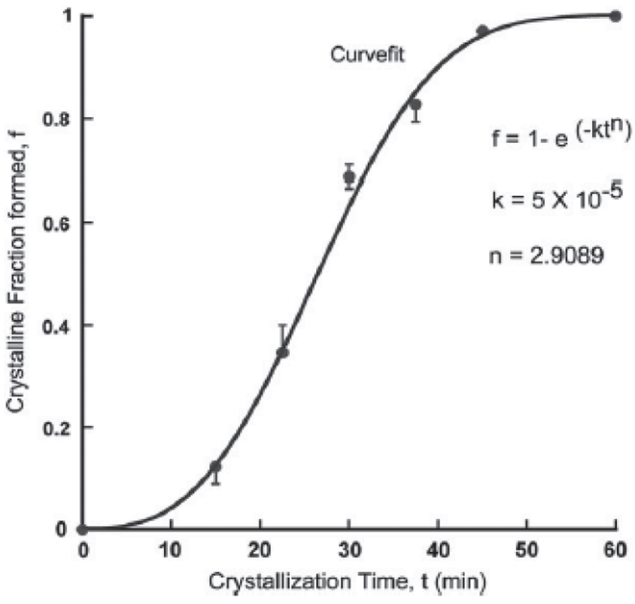

Figure 5: Crystallization fraction V/s crystallization time, (showing the crystallization of Bioglass 45S5 at 680°C)[26].

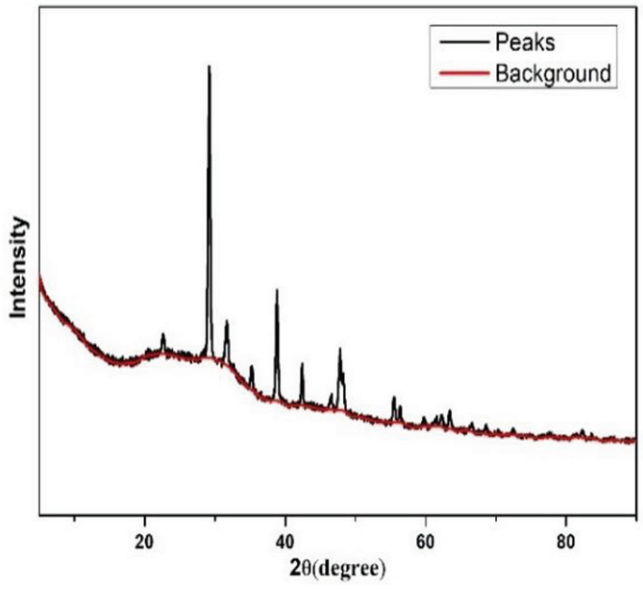

Figure 6: XRD pattern showing background corresponding to amorphous phase and peaks corresponding to crystallinity phase in bioglass

it is said to bulk crystallization with three-dimensional crystal growth take place [26].

3.1.3 X-Ray Diffraction Analysis (XRD)

The crystallization behaviour can be determined by XRD analysis using X-ray diffractometer in the range of 10° to 80° and step size of 0.02° with Cu kα radiation. the crystalline phases can be determined by Xpert High Score software. The XRD revels the different crystalline phases and compositional changes that occurs under the influence of thermal treatment. The presence of different silicate phases (such as, $Na_2Ca_2Si_3O_9$, $Na_2CaSi_2O_6$, $Na_2Ca_2(Si_3)_3O_9$ and Na_2CaSiO_4) and calcium silicate phosphate (such as $Ca_5(PO_4)_2SiO_4$, $Na_2Ca_4(PO_4)_2SiO_4$ and sili-corhenanite) were identified in the XRD pattern [5,30]. Particularly orthophosphate ions induce in the formation of phosphate-rich crystalline phases [23]. Thus, it says the evolution of crystalline phases are the function of time and temperature. Fig.6 shows the XRD pattern of solgel synthesized bioglass sample, stabilised at 600°C with background and peak intensity representing the amorphous and crystalline phases. These XRD patterns are used to calculate the degree of crystallinity by following equation (5).

$$\%\ of\ crystallinity = \frac{Ig-Ix}{Ig-Ib} \times 100 \quad \text{... (5)}$$

Where, I_g is the non-crystalline intensity, I_x is the partially crystallized intensity, I_b is the background correction obtained for air, instrument and Crompton effect [19,1]. Similarly, Prakrathi et.al. demonstrated a method to evaluate the rate of crystallization during stabilisation by using I_{PB} ratio, which is the ratio of integral area of background to integral area of peaks and the method is used for evaluating rate constant of the reaction (devitrification reaction) [27]

Table 1: Evolution of crystalline phases as a function of time and temperature [23]

Relative amount (wt.%)	Sintering temp. 600°C and time			
	at 0.5hr	at 1hr	at 2hr	at 4hr
Combeite	30.6	44.6	74.2	72.5
$NaNO_3$	39.2	37.3	14.5	13.2
$Na_2Ca_2Si_2O_7$	-	-	-	-
Rhenanite	-	-	11.3	14.3
$Ca_{15}(PO_4)_2(SiO_4)_6$	30.2	18.2	-	-
	Sintering temp. 700°C and time			
Combeite	75.8	73.3	77.0	81.3
$NaNO_3$	2.6	2.5	1.2	1.5
$Na_2Ca_2Si_2O_7$	21.5	24.9	21.9	17.2
Rhenanite	-	-	-	-
$Ca_{15}(PO_4)_2(SiO_4)_6$	-	-	-	-

4.0 New Insights Into Crystallization of Bioglass

The data in the Table 1 was obtained from XRD rietveld refinement analysis, results which tell us temperature and time of sintering process influence the formation of crystalline phase. At 600°C, the main phase formed is combeite along with secondary phases (such as, rhenanite, $NaNO_3$ and calcium-silicate- phosphate). The results indicated that combeite and rhenanite phase are increased with decomposition of $NaNO_3$ and $Ca_{15}(PO_4)_2(SiO_4)_6$ with increase in time duration. At 700°C, the main phase combeite will keep on increasing with decomposition of $NaNO_3$ and rhenanite that leads to formation of new crystalline phase like sodium calcium silicate ($Na_2Ca_2Si_2O_7$). As the table indicates crystalline phases can be tailored by controlling nucleation and growth through sintering process.

5.0 Conclusions

In this review it provides a literature overview of different application of bioglass prepared by solgel and melt-quench techniques. Different heating rate can influence the crystallization. From the Avrami equation we can determine the type of crystallization occurs at different rate of heat treatment and also the activation energy and Avrami exponent which helps in finding out the crystallization event. The structural transition of bioglass can be determined by DSC/DTA analysis. The microscopic analysis helps in finding out the micropores and macropore which influence the crystallinity of the bioglass. From XRD analysis we can obtain the percentage of crystallinity occurred in the bioglass. Concluding by say that crystalline phases can be controlled and tailored through heat treatment process.

6.0 Reference

[1] A.Z. Karimi et al. .., 0022-3093.
[2] Bellucci D. et al. .., 2014. C, 43, pp.573- 586.
[3] Boccaccini et al. .., 2007. 136, pp.27-44.
[4] Bretcanu et al. .., 2009. 29(16), pp.3299-3306.
[5] Cacciotti et al. .., 2012.23(8), pp.1849-1866.
[6] Cannio M. et al. ...,2021 14(18), p.5440.
[7] Cattini A et al. .., 2013. 220, pp.52-59.
[8] Doweidar H et al. .., 2009. 355(9), pp.577-580.
[9] F.J. Hmood et al. .., 2020. 6. 3, p.100027.
[10] Hench L.L et al. .., 2011. 25.
[11] Jaimes et al. .., 2021. 41(9), pp.4958-4969.
[12] Jones, J.R. 9(1), pp.4457-4486.
[13] K. Zheng et al. .., 2015.98(1), pp.30-38.
[14] Kokubo T. et al. .., 1991.12(2), pp.155- 163.
[15] L. Lefebvre et al. .., 2007, 55, 3305–3313.
[16] Li R. et al. ..,1991. 2(4), pp.231-239.
[17] Manda et al. .., 2012. 38(7), pp.5585-5596.
[18] Nawaz et al. .., 2021.41(2), pp.1695-1706.
[19] Ohlberg S.M. and Strickler D.W., 1962. 45(4), pp.170-171.
[20] P.Paramita et al. .., 2021. 32(1), pp.1-11.
[21] Pirayesh H. and Nychka, J.A., 2013. 96(5), pp.1643-1650.
[22] Plewinski M. et al. .., al., 2013. 29(12), pp.1256-1264.
[23] Q. Nawaz. et al. .., 2020.103(8), pp.4234- 4247.
[24] R.R. Chandran et al. .., 2021. 45(34), pp.15350-15362.
[25] Ramila A et al. ..,2002.14(2), pp.542-548.
[26] S. Kashyap et al. .., 2011.31, 762-769.
[27] S. Prakrathi et al. .., 2018, p.020091.
[28] Sepulveda P et al. .., 2001. 58(6), pp.734-740.
[29] Vallet Regí M et al. .., 2016.7(2), pp.195- 205.
[30] X.Liu et al. .., 2013. 9(6), pp.7025-7034.